Phase coherent transport in $SrTiO_3/LaAlO_3$ interfaces

D. Rakhmilevitch, M. Ben Shalom, M. Eshkol, A. Tsukernik, A. Palevski, and Y. Dagan*
Raymond and Beverly Sackler School of Physics and Astronomy, Tel-Aviv University, Tel Aviv 69978, Israel
(Received 7 September 2010; revised manuscript received 6 November 2010; published 14 December 2010)

The two-dimensional electron gas formed between $SrTiO_3$ and $LaAlO_3$ exhibits a variety of interesting physical properties which make it an appealing material for use in future spintronics and/or quantum-computing devices. For this kind of applications electrons have to retain their phase memory for sufficiently long times or length. Using a mesoscopic size device we were able to extract the phase coherence length, L_ϕ, and its temperature variation. We find the dephasing rate to have a power-law dependence on temperature. The power depends on the temperature range studied and sheet resistance as expected from dephasing due to strong electron-electron interactions.

DOI: 10.1103/PhysRevB.82.235119 PACS number(s): 75.47.−m, 73.20.Fz, 73.23.−b, 73.40.−c

I. INTRODUCTION

Oxides interfaces have recently attracted considerable scientific attention due to their potential for implementation in oxide-based electronics and for basic science. One of the most studied examples is the interface between $LaAlO_3$ and $SrTiO_3$ (LAO/STO).[1] In this interface a highly conducting two-dimensional electron gas (2DEG) appears above a critical thickness of 4 unit cells (uc).[2]

Magnetotransport in the 2DEG formed at the interface between STO and LAO exhibits quite rich behavior in low and high magnetic fields in both perpendicular and parallel orientations.[3] The magnetoresistance at low magnetic fields was described in terms of suppression of weak localization.[4] However, it is difficult to sort out the contribution of quantum corrections to the magnetoresistance from other possible mechanisms such as two types of charge carriers and inhomogeneities. Therefore, there is a need for a different type of measurement sensitive solely to the mesoscopic phase coherence, such as universal conductance fluctuations (UCF).[5–7] The observation of UCF is therefore a direct proof for the importance of quantum corrections to the conductance at low temperatures for STO/LAO interfaces.

It has been shown that the conductivity of sample with a given impurity concentration will fluctuate around its average value upon changing the impurity configuration. For two dimensions these fluctuations should have a universal value on the order of $\frac{e^2}{h}$.[5] An experimental realization simulating such a configuration modification is achieved by an application of external magnetic field.[8] In this case the magnetoconductance will produce a reproducible fluctuating curve. In order to observe this effect the size of the sample should be comparable with the low-temperature length scales: L_ϕ, the phase breaking length and/or $L_T=\sqrt{\frac{hD}{k_BT}}$ the so-called thermal length. The root-mean-square (rms) value of the UCF and the width of the typical oscillation provide information on L_T and L_ϕ when the length and the width of the sample exceed the above microscopic lengths.[9,10]

For a macroscopic sample the UCF average out. However, coherent back scattering also known as weak localization (WL) (Refs. 11–13) still affects the conductance. The latter quantum corrections as well as the UCF depend on the same microscopic length scale, L_ϕ. The observation of both the WL and UCF with a similar L_ϕ can provide a strong evidence that the low-field magnetoresistance in macroscopic samples is governed by quantum-interference effects.

In this paper, we report studies of magnetoconductance fluctuations in mesoscopic samples of the 2DEG at the STO/LAO interface as well as WL in a macroscopic sample. The analysis of the UCF suggests that the low-field magnetoresistance for macroscopic samples at the low-carrier densities is governed by quantum corrections, namely, weak localization. In addition, we show that for these densities the dephasing mechanism is mainly due to electron-electron interactions.

II. SAMPLE PREPARATION AND MEASUREMENTS

LAO layers were epitaxially grown on atomically flat TiO_2-terminated STO substrates using pulsed laser deposition. The growth parameters are described elsewhere.[3] Hall-bar patterns were created using a combination of photo- and electron-beam lithography. The LAO was dry etched using Ar ions. The etching was followed by a short oxygen treatment at 200 °C in order to anneal out oxygen vacancies created in the substrate during the etching.

In order to observe the UCF we used a sample characterized by low-sheet resistance (sample A). The dimensions of the Hall bar used are 4 μm × 1.5 μm. The temperature dependence of the localization peak was studied on a sample with a higher sheet resistance (sample B). We use a large sample (5×5 mm^2) in a Van der Pauw configuration to eliminate the effect of the UCF. The sheet resistance was tuned using the thickness of the LAO layer,[14] 8 unit cell and 20 unit cell for the low (sample A) and high (sample B) sheet resistances, respectively.

III. RESULTS AND DISCUSSION

A. Observation and analysis of the universal conductance fluctuations

The typical magnetoresistance curve of the bridge is shown in Fig. 1(a). The field was cycled from −4 to 4 T for several times at 1.3 K and at 4.2 K. Two of these traces at 1.3 K are shown. A reproducible fluctuating signal is clearly seen. These are the universal conductance fluctuations. Fig-

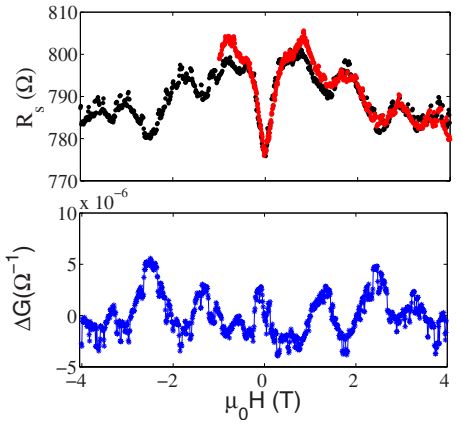

FIG. 1. (Color online) (a) Sheet resistance versus magnetic field of sample A at 1.3 K. Two traces of the magnetic field sweep are shown (red circles and black squares) note the reproducible fluctuations pattern. (b) The deviation of the magnetoconductance from its average value (see text for details).

ure 1(b) shows conductance deviations from its average as a function of field. The subtracted average background magnetoconductance is obtained by removal of the WL fit plotted in Fig. 2.

The conductance-correlation function

$$F(\Delta B) = \langle \delta g(B)\delta g(B+\Delta(B)\rangle \tag{1}$$

was calculated from the data in Fig. 1(b). $F(\Delta B=0)$ gives the rms value of the fluctuations. The magnetic correlation field B_c is found from

$$F(\Delta B = B_c) = \frac{1}{2}F(\Delta B = 0). \tag{2}$$

For sample dimensions L with $L > L_\phi \approx L_T$ the rms value is given by[15–17]

$$\delta G = \frac{N_v \alpha}{\beta} \times \frac{e^2}{h} \times \sqrt{\frac{4W}{\pi L^3}} \times L_\phi, \tag{3}$$

where β represents the effect of SO coupling on the size of the fluctuations. β goes to 2 at the strong-coupling limit.[15] The $N_v\alpha$ factor stands for the effect of valley degeneracy and

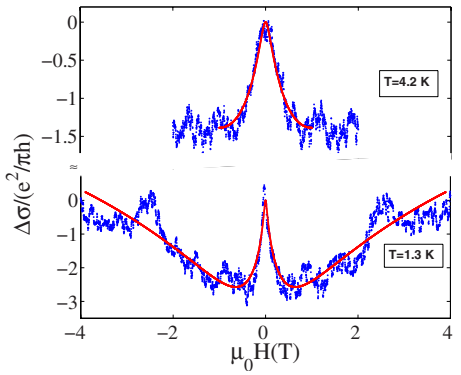

FIG. 2. (Color online) Magnetoconductance at 1.3 K and at 4.2 K for sample A. The solid lines are fits to Eq. (5).

is the same as the factor that appears in weak localization theory.[16] α has been theoretically predicted to be of order 1. From this relation using our measured rms value and the known sample dimensions we find $L_\phi = 1570 \pm 300$ Å at 1.3 K. Here we assume that spin-orbit scattering length, L_{so} is much shorter than the dephasing length L_ϕ and therefore $\beta \approx 2$. This is reasonable in view of the strong spin-orbit coupling observed in this material.[18] The valley degeneracy N_v is assumed to be 3 as in bulk STO.[19] The consistency of this assumption as well as the assumption $L_\phi \approx L_T$ will be addressed further below.

The dependence of B_c on L_ϕ has been calculated[17]

$$L_\phi = \sqrt{\frac{h/e}{B_c}}. \tag{4}$$

For $L_\phi \approx L_T$. Substituting the obtained value for B_c we find $L_\phi = 1650 \pm 320$ Å, consistent with the value estimated from the rms value of the fluctuation amplitude.

B. Temperature dependence of the phase coherence length

The magnetoconductance dip at zero magnetic field was analyzed in the framework of WL theory in the presence of spin-orbit interactions.[20,21] The data and the theoretical curves using Eq. (5) are presented in Fig. 2

$$\Delta\sigma(H,T)_{\mathrm{WL}} = \frac{e^2}{\pi h} N_v \alpha \left[\Psi(x_1) + \frac{1}{2\sqrt{1-\gamma^2}}\Psi(x_2) - \frac{1}{2\sqrt{1-\gamma^2}}\Psi(x_3) \right], \tag{5}$$

where

$$\Psi(x) = \ln(x) + \psi\left(\frac{1}{2}+\frac{1}{x}\right), \quad x_1 = \frac{H}{H_i + H_{so}},$$

$$x_2 = \frac{H}{H_i + H_{so}(1+\sqrt{1-\gamma^2})}, \quad x_3 = \frac{H}{H_i + H_{so}(1-\sqrt{1-\gamma^2})}$$

$\gamma = g\mu H/(4eDH_{so})$ and $N_v = 3$.[19] We used $\alpha \approx 1$ as theoretically predicted for intervalley scattering rate smaller than the dephasing one[22] and $g = 2.25$ consistent with Ref. 4 for sample with a similar sheet resistance. $L_\phi(T)$ and L_{so} are used as the fitting parameters.[23] From the fit we find $L_\phi = 1300 \pm 260$ Å consistent with the values found from UCF and $L_{so} \approx 200$ Å. L_{so} is indeed significantly shorter than L_ϕ at 1.3 K as we assumed earlier in the analysis of the UCF data. It is important to stress that the value of L_ϕ deduced from the fit to the WL calculations is similar to that extracted from the UCF. This provides an important evidence that weak localization corrections play an important role in the low-field magnetotransport.

At 4.2K $L_\phi = 640 \pm 100$ Å. It is much shorter than at 1.3 K. We note that the ratio of the diffusion coefficient for these temperatures is $\frac{D(4.2K)}{D(1.3K)} = \frac{R(1.3K)}{R(4.2K)} = 1.5$. Since $L_\phi = \sqrt{D\tau_\phi}$ we obtain $\frac{\tau_\phi(4.2K)}{\tau_\phi(1.3K)} = 6$, much higher than the ratio between the phase coherence lengths. In order to elucidate the mechanism responsible for dephasing we carefully studied the temperature

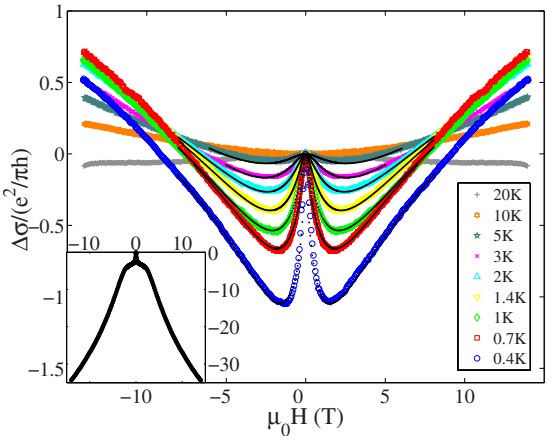

FIG. 3. (Color online) The normalized magnetoconductance for sample B at various temperatures. The solid lines are fits to Eq. (5). Inset: the normalized magnetoconductance at 0.4 K for sample with 8 uc having a higher mobility.

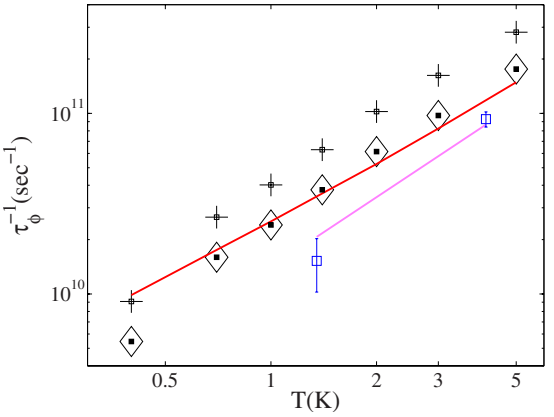

FIG. 4. (Color online) The dephasing rate extracted from the fits in Figs. 2 and 3 for sample A with $m^*=3m_e$ (squares), and for sample B using $m^*=3m_e$ (crosses) and $m^*=5m_e$ (diamonds). The lines are the theoretical curve using Eq. (6).

dependence of the magnetoresistance. We used the macroscopic sample (sample B) since in such a sample the analysis of the central weak localization feature is less affected by the UCF themselves, which can alter the conductance at low fields. In addition for this sample the WL peak is pronounced and can be followed in a wide temperature range. In principle, one could study a mesoscopic sample but for our case the number of fluctuations is too small to provide an accurate measurement for the temperature dependence of L_ϕ.

In Fig. 3 we present the magnetoconductance curves for sample B for temperatures ranging from 0.35 to 20 K. The solid lines are the theoretical fits using Eq. (5). Here we also used $L_\phi(T)$ and L_{so} as the fitting parameters. The data was fit for a field range between −5 to 5 T (or more). The higher field region was not included in the fit to avoid high-field contributions due to electron-electron interactions and other possible corrections.[24] The fit is excellent for $T<5$ K where quantum corrections dominate the low-field behavior. For this sample we used $g=0.6\pm0.1$ (consistent with Ref. 4 for similar sheet resistance). We allowed g to vary within the error bar for the various temperatures to obtain a better fit for the higher field regime. This small variation does not effect the value of L_ϕ. The data could not be fit with $N_v\alpha=3$ but with $N_v\alpha=1$. The diminished role of the valley degeneracy for this sample can be explained by a stronger intervalley scattering.[22,25] We should keep in mind that this sample has mobility ≈6 times lower than sample A. In addition, $\alpha N_v=1$ was also used in Ref. 4 for samples with similar sheet resistance. We note that while the magnetoresistance can be well explained by Eq. (5) the temperature dependence of the resistivity is more complicated. Other effects not included in our simple analysis may be involved. However, since the localization peak is seen together with the UCF we can be sure that quantum corrections dominate the magnetoconductance at low temperatures.

In the insert of Fig. 3 the normalized magnetoconductance for an 8 uc sample (sample C) at 0.4 K is presented. As expected from the lower thickness, the mobility is larger for this sample and the sheet resistance is lower. Consequently the localization peak is a small feature overwhelmed by the large magnetoresistance (typical for these samples). In addition, the spin-orbit peak cannot be resolved even at this low temperature. Since one of the biggest achievements of mesoscopic physics is the ability to predict the transport properties of any (mesoscopic) sample with given dimensions based solely on its conductance or sheet resistance we believe that our analysis for samples A and B is valid despite the difference in LAO overlayer thickness.

C. Analysis of the dephasing rate

The quasielastic electron-electron-scattering time is known to be dependent on disorder. At low temperatures, in most cases, this is the major mechanism for the dephasing. This can explain the difference in dephasing between the two samples. To verify this assumption we plot the dephasing rate as function of temperature for both samples.

In Fig. 4 the dephasing rate calculated from $L_\phi=\sqrt{D\tau_\phi}$ is plotted as a function of temperature on a logarithmic scale for both samples. The diffusion coefficient was calculated from Einstein relation $D=\frac{\pi\hbar^2}{N_v m^* e^2 R_\square}$. We used an effective mass of $m^*=3m_e$ (m_e the bare electron mass) and $N_v=3$ as found for bulk $SrTiO_3$. A linear temperature dependence is observed for sample B. The dephasing rate extrapolates to zero at zero temperature. This temperature dependence is expected from a Nyquist noise resulting from electron-electron interactions. For sample A a higher exponent is observed. Narozhny *et al.*[26] calculated the dephasing rate for this case and found it to depend on the sheet resistance. This theory well describes the dephasing rate in semiconductors.[27]

$$\frac{1}{\tau_\phi}=\left\{1+\frac{3(F_0^\sigma)^2}{(1+F_0^\sigma)(2+F_0^\sigma)}\right\}\frac{k_BT}{\eta\hbar}\ln[\eta(1+F_0^\sigma)]+\frac{\pi}{4}\left\{1+\frac{3(F_0^\sigma)^2}{(1+F_0^\sigma)^2}\right\}\frac{(k_BT)^2}{\hbar E_F}\ln(E_F\tau/\hbar), \quad (6)$$

where F_0^σ is the interaction constant in the triplet channel, which depends on interaction strength,[28] $\eta=\frac{2\pi\hbar}{e^2R_\square}$, k_B is the Boltzmann constant, and E_F is the Fermi energy.

The solid lines in Fig. 4 are theoretical curves for the dephasing rate using the measured parameters for our samples. We used $F_0^\sigma=0$ for both samples since the interaction parameter r_s is expected to be small. The dephasing rate calculated from the data of sample B fits the theoretical curve using $m^*=5m_e$ (Ref. 29) we also show $\frac{1}{\tau_\phi}$ for $m^*=3m_e$. Since the theoretical calculation is accurate within a factor of 2 one can safely state that both sets of τ_ϕ^{-1} agree with the theoretical curve. The dephasing rate for sample A at 1.3 K $\tau_\Phi^{-1}\approx 2.1\times 10^{10}$ s^{-1} which is indeed very close to $\frac{k_BT}{h}\approx 2.7\times 10^{10}$ S^{-1} thus justifying the assumption of $L_\phi\approx L_T$ use in the UCF analysis.

For sample B the sheet resistance is high, therefore the first term in Eq. (6) dominates. This term gives the observed linear temperature dependence. For sample A the sheet resistance is three times lower. Consequently the quadratic term has a significant contribution for the temperature range studied. The fact that data fit the theoretical curves put strong limitations on the product $N_v m^*$, which appears in the diffusion coefficient. Moreover, it can be seen in Eq. (6) that for low-resistance samples the temperature dependence of the dephasing rate depends on the Fermi energy and hence on the product $N_v m^*$ (α does not enter into the calculation of τ_ϕ). The importance of the quadratic term in our data (sample A) can therefore provide additional information on the effective mass. Hence we can conclude that $N_v m^*$ should be very close to $9m_e$. If we assume that m^* is very large (say $m^*=9$ and $N_v=1$) it will be difficult to explain the absence of a quadratic term in the dephasing rate for sample B. If m^* is small the measured dephasing rate will go below the theoretical limit set by the Nyquist noise. We therefore conclude that m^* is on the order of a few m_e. Similar results were obtained from infrared ellipsometry.[30]

IV. SUMMARY

We measured universal conductance fluctuations in a mesoscopic sample of $LaAlO_3/SrTiO_3$ interface. The phase coherence length obtained from these fluctuations equals (within the error) to that found from fitting the low-field magnetoresistance curves. This suggests that the magnetoresistance at low fields is dominated by quantum corrections. We analyze the temperature dependence of the magnetoresistance in terms of the weak-localization theory. From the temperature dependence of the dephasing rate we conclude that it is dominated by electron-electron interactions. The dephasing time fits very well to the theoretical calculations of Narozhny *et al.*[26] assuming an effective mass of $3m_e$. Since dephasing time is only limited by electron-electron interactions it seems that increasing the carrier concentration by gate voltage application will enhance the phase coherent length over the micrometer scale, meeting the requirements of quantum-coherent electronic devices.

ACKNOWLEDGMENT

This research was supported by the Israel Science Foundation F.I.R.S.T program under Grants No. 1543/08 and No. 1421/08.

*yodagan@post.tau.ac.il

[1] A. Ohtomo and H. Y. Hwang, Nature (London) **427**, 423 (2004).
[2] S. Thiel, G. Hammerl, A. Schmehl, C. W. Schneider, and J. Mannhart, Science **313**, 1942 (2006).
[3] M. Ben Shalom, C. W. Tai, Y. Lereah, M. Sachs, E. Levy, D. Rakhmilevitch, A. Palevski, and Y. Dagan, Phys. Rev. B **80**, 140403 (2009).
[4] A. D. Caviglia, M. Gabay, S. Gariglio, N. Reyren, C. Cancellieri, and J.-M. Triscone, Phys. Rev. Lett. **104**, 126803 (2010).
[5] A. D. Stone, Phys. Rev. Lett. **54**, 2692 (1985).
[6] A. Benoit, C. P. Umbach, R. B. Laibowitz, and R. A. Webb, Phys. Rev. Lett. **58**, 2343 (1987).
[7] W. J. Skocpol, P. M. Mankiewich, R. E. Howard, L. D. Jackel, D. M. Tennant, and A. D. Stone, Phys. Rev. Lett. **56**, 2865 (1986).
[8] P. A. Lee and A. D. Stone, Phys. Rev. Lett. **55**, 1622 (1985).
[9] P. A. Lee, A. D. Stone, and H. Fukuyama, Phys. Rev. B **35**, 1039 (1987).
[10] T. J. Thornton, M. Pepper, H. Ahmed, G. J. Davies, and D. Andrews, Phys. Rev. B **36**, 4514 (1987).
[11] E. Abrahams, P. W. Anderson, D. C. Licciardello, and T. V. Ramakrishnan, Phys. Rev. Lett. **42**, 673 (1979).
[12] B. L. Altshuler, D. Khmel'nitzkii, A. I. Larkin, and P. A. Lee, Phys. Rev. B **22**, 5142 (1980).
[13] G. Bergmann, Phys. Rev. Lett. **48**, 1046 (1982).
[14] C. Bell, S. Harashima, Y. Hikita, and H. Y. Hwang, Appl. Phys. Lett. **94**, 222111 (2009).
[15] V. Chandrasekhar, P. Santhanam, and D. E. Prober, Phys. Rev. B **42**, 6823 (1990).
[16] R. G. van Veen, A. H. Verbruggen, E. van der Drift, F. Schffler, and S. Radelaar, Semicond. Sci. Technol. **14**, 508 (1999).
[17] B. Z. Spivak and A. Y. Zyuzin, *Mesoscopic Phenomena in Solids* (Elsevier, Amsterdam, 1991), Vol. 30.
[18] M. Ben Shalom, M. Sachs, D. Rakhmilevitch, A. Palevski, and Y. Dagan, Phys. Rev. Lett. **104**, 126802 (2010).
[19] H. P. R. Frederikse, W. R. Hosler, W. R. Thurber, J. Babiskin, and P. G. Siebenmann, Phys. Rev. **158**, 775 (1967).
[20] S. Hikami, A. I. Larkin, and Y. Nagaoka, Prog. Theor. Phys. **63**, 707 (1980).
[21] S. Maekawa and H. Fukuyama, J. Phys. Soc. Jpn. **50**, 2516 (1981).
[22] H. Fukuyama, Prog. Theor. Phys. **69**, 220 (1980).
[23] It is reasonable to assume temperature independent spin-obit coupling if it is Rashba type. In addition, the dielectric constant does not change below 10 K.
[24] P. A. Lee and T. V. Ramakrishnan, Rev. Mod. Phys. **57**, 287 (1985).
[25] S. Kawaji, Prog. Theor. Phys. **84**, 178 (1985).
[26] B. N. Narozhny, G. Zala, and I. L. Aleiner, Phys. Rev. B **65**, 180202 (2002).

[27] M. Eshkol, E. Eisenberg, M. Karpovski, and A. Palevski, Phys. Rev. B **73**, 115318 (2006).

[28] G. Zala, B. N. Narozhny, and I. L. Aleiner, Phys. Rev. B **64**, 214204 (2001).

[29] The notable deviation of the dephasing rate at 0.4 K from the theoretical prediction could be attributed to a suppression of the superconducting fluctuations by the magnetic field at low temperatures.

[30] A. Dubroka, M. Rössle, K. W. Kim, V. K. Malik, L. Schultz, S. Thiel, C. W. Schneider, J. Mannhart, G. Herranz, O. Copie, M. Bibes, A. Barthélémy, and C. Bernhard, Phys. Rev. Lett. **104**, 156807 (2010).